Comparison of the Structure and Properties of Liposomes Prepared from Milk Fat Globule Membrane and Soy Phospholipids

ABBY K. THOMPSON,[†] JASON P. HINDMARSH,[†] DEREK HAISMAN,[†]
THOMAS RADES,[§] AND HARJINDER SINGH*,[†]

Riddet Centre, Massey University, Palmerston North, New Zealand, and National School of Pharmacy,
University of Otago, Dunedin, New Zealand

Liposomes were prepared from a milk fat globule membrane (MFGM) phospholipid fraction and from soy phospholipid material using a high-pressure homogenizer (Microfluidizer). The liposomes were characterized in terms of general structure, phase transition temperature, lamellarity, bilayer thickness, and membrane permeability. The liposomes prepared from the MFGM fraction had a significantly higher phase transition temperature, thicker membrane, and lower membrane permeability. These differences were attributed to different phospholipid compositions of the MFGM and soy phospholipid fractions.

KEYWORDS: Encapsulation; liposome; Microfluidizer; milk fat globule membrane; MFGM; phospholipid

INTRODUCTION

Liposomes are spherical structures consisting of one or more phospholipid bilayers enclosing an aqueous core (*1*) and are generally produced from highly purified phospholipids extracted from soy oil or egg yolk. These structures may be used for a wide variety of applications, including the entrapment and controlled release of drugs or nutraceuticals and as model cells or membranes (*2*). There are a large number of potential opportunities for use of liposomes in the food industry (*1*, *3−15*), but the high cost of the soy and egg phospholipids used by the pharmaceutical industry has limited their commercial application in food systems.

Recent research into the biological functions of phospholipids and sphingolipids has identified a number of health benefits, including liver protection (*16*), memory improvement (*17*, *18*), and inhibition of cholesterol absorption (*19*). This has sparked interest in producing a valuable product through the isolation of the milk fat globule membrane (MFGM) phospholipids and sphingolipids present in waste dairy streams such as buttermilk (*20*, *21*). The emulsifying properties of this material have been previously discussed (*22*, *23*), and emulsions produced from MFGM fractions have been successfully used for the delivery of drugs (*24*, *25*). Recently, we reported that MFGM-derived phospholipids can also be used to produce liposomes by microfluidization (*26*).

Like all natural sources of phospholipid material, MFGM-derived fractions contain a number of different classes of phospholipids. The zwitterionic phosphatidylcholine (PC), phosphotidylethanolamine (PE), and sphingomyelin (SM) each constitute between 20 and 40% of the phospholipid in the MFGM, with smaller amounts of the anionic phosphatidylserine (PS) and phosphatidylinositol (PI) also present (*20*, *27*). The primary phospholipid components of soy lecithin are PC, PE, and PI, the specific quantities of each class being a function of the processing technique (*28*). The fatty acid profile of the chains attached to the phospholipid headgroups also varies between the different phospholipid source materials, with MFGM-derived fractions tending to be more highly saturated than their soy counterparts (*14*, *29*). The unique composition of the MFGM phospholipid material (in particular, the high proportion of sphingolipids) may result in liposomes with different properties as well as provide nutritional benefit for the consumer. Waninge et al. (*30*) showed that liposome-like vesicles could be produced out of simulated MFGM phospholipids, and our previous paper has revealed that liposomes can also be manufactured from MFGM material commercially isolated from buttermilk (*26*).

At a basic level, measuring the average size and size distribution of the liposome population is essential, but a more thorough characterization involves a number of properties that may provide an indication of likely entrapment and release kinetics and the stability of the system (*31*). The phase transition temperature of a liposome population directly affects membrane permeability at different temperatures and hence the rate of release of entrapped material (*1*). The thickness of the bilayer membrane is likely to affect diffusion rates, as is lamellarity, with multilamellar liposomes thought to provide a more gradual and sustained release compared with unilamellar liposomes (*32*). The surface charge is often related to stability due to electrostatic

* Address correspondence to this author at the Riddet Centre, Massey University, Private Bag 11 222, Palmerston North, New Zealand (telephone +64 6 356 4401; fax + 64 6 350 5655; e-mail h.singh@massey.ac.nz).
† Massey University.
§ University of Otago.

Structure and Properties of Liposomes

J. Agric. Food Chem., Vol. 54, No. 10, 2006 **3705**

interactions between the liposomes, which are important as destabilization of the system often leads to loss of entrapped material (*7*).

This paper extends our previous studies (*26*) and compares the composition of MFGM- and soy-derived phospholipid fractions and evaluates the physical and chemical characteristics of liposome dispersions produced from the two materials using microfluidization.

MATERIALS AND METHODS

A MFGM-derived fraction rich in phospholipids (Phospholac 600) was provided by the Fonterra Co-operative Group Ltd. (New Zealand). A purified soy phospholipid fraction (Sigma product P3644, minimum 30% phosphatidylcholine, Sigma-Aldrich, St. Louis, MO) was also used to allow comparisons between liposomes produced from the different phospholipid sources. All chemicals used were of analytical grade and obtained from Sigma-Aldrich.

Characterization of Phospholipid Material. *Proximate Analysis.* A basic proximate analysis of the samples of phospholipid powders was undertaken to provide information on the overall composition of the fractions.

Moisture was determined in triplicate by the loss in weight of powder dried at 105 °C for 24 h in an air oven.

The ash content was determined by dry ashing, where the powder was heated in a muffle furnace at 550 °C for 5 h, cooled in a desiccator, and weighed. The mineral content was determined in more detail using an acid digest and inductively coupled plasma optical emission spectrometry (ICP-OES) (AgriQuality, Auckland, New Zealand).

The triglyceride content of the phospholipid powders was measured using a triglyceride diagnostic kit (Roche Diagnostics Ltd., Basel, Switzerland; catalog no. 2016648). The concentration of phospholipid in the fractions (grams per kilogram) was calculated on the basis of the amount of phosphorus present, as determined using ICP-OES, using an average phospholipid molecular weight (M_r) of 775 (*33, 34*). It was assumed that there was no free phosphorus or other entities that contained phosphorus present in the sample.

The crude protein content of foods is usually derived by multiplying the nitrogen content by an empirical conversion factor. However, the presence of nitrogen in each of the phospholipid fractions means that this approach cannot be used. Therefore, the ratio of nitrogen to phospholipid was used to provide an indication of the relative amount of protein in the samples. The nitrogen content of the samples was determined according to the Kjeldahl method (AOAC official method 991.20). The samples and blank were digested at 220 °C for 60 min in a Kjeltec 1030 System (Tecator, Sweden).

The amount of cholesterol present in the phospholipid fractions was measured using gel chromatography based on the AOAC official methods 933.08, 970.50, and 970.51 (AgriQuality, Auckland, New Zealand).

Phospholipid Headgroup. [31]Phosphorus nuclear magnetic resonance (^{31}P NMR) analysis was performed by Spectral Service (Köln, Germany) on the phospholipid material in its original powder state using a Bruker AC-P 300 MHz NMR spectrometer (*35, 36*).

Fatty Acid Profile. The lipid was extracted from the phospholipid powders using chloroform and methanol in a ratio of 1:2 (v/v). Fatty acids were methylated via acid-catalyzed transesterification at 80 °C for 12 h in a sealed tube. The fatty acid methyl esters were separated using a BPX-70 capillary column, 100 m × 0.22 mm i.d., 0.25 μm film (SGE, Melbourne, Australia). The gas chromatographic system consisted of a 6890 gas chromatograph equipped with an autosampler (HP7673) and Chem Station integration (all Hewlett-Packard, Avondale, PA). The column oven was held at 165 °C for 52 min and then increased at a rate of 5 °C/min to 210 °C for 59 min (total run time = 120 min). The injector port and the flame ionization detector port were both held at 250 °C. The carrier gas (helium) flow rate was 1.0 mL/min (linear gas velocity = 20 cm/s), with an inlet split ratio of 30:1. Fatty acid peaks were identified by matching the retention time with those of authentic standards, including a composite standard made from com-

mercially available methyl esters (NuCheck Prep, Elysian, MN; and Sigma, St. Louis, MO).

Preparation of Liposomes. The phospholipid powders were dispersed in imidazole buffer (20 mM imidazole, 50 mM sodium chloride, and 0.02% sodium azide in Milli-Q water, adjusted to pH 7, with 1 M hydrochloric acid) and thoroughly mixed using a JKA Ultra-Turrax (JKA, Staufen, Germany) to produce a dispersion with a phospholipid concentration of 10% (w/w). The phospholipid dispersion was then passed through a M-110Y Microfluidizer (Microfluidics International Corp., Newtown, MA) with a 75 μm F12Y-type interaction chamber five times at ~1100 bar (17000 psi).

Characterization of Liposomes. *Average Size and Size Distribution of Liposomes.* The average hydrodynamic diameter of the liposome dispersions was measured by photon correlation spectrometry (PCS) using a Zetasizer 4 (Malvern Instruments Ltd., Worcestershire, U.K.). The liposome dispersions were diluted to the required turbidity (<250 kcps) with imidazole buffer, and samples were analyzed in triplicate at 25 °C with a sampling time of 99 s and a scattering angle of 90°. A typical refractive index of 1.45 for a liposome (*37, 38*) was used, with a medium viscosity of 1.054 cP and a refractive index of 1.34 for the aqueous phase.

Asymmetrical flow field-flow fractionation (AFFF) was performed using a Postnova Avalanche AF4 AFFF (Postnova, Munich, Germany) equipped with a Postnova refractive index detector (PN 3140) and a Precision Detectors PD Expert multiangle dynamic and static light-scattering system (www.precisiondetectors.com). The channel outlet flow was held constant at 0.3 mL/min with a channel spacer of 0.25 mm. A field programming method using power field decay was used, with the field held constant at 70% for 4.8 min and then decaying at the rate of $-p \times 4.8$ min, where $p = 2$. This method was designed to give the optimum separation in 60 min for particles between 7.5 and 750 nm in diameter, providing a more detailed analysis of the size distribution of the liposome dispersions.

Electron microscopy. Two different electron microscopy techniques were used to provide information on the microstructure of the liposome dispersions: negative staining transmission electron microscopy (TEM) and cryofield emission scanning electron microscopy (cryo-FESEM).

The negative staining TEM required the liposome dispersions to be diluted ~ 1:10 with distilled water to reduce the concentration of the liposomes. Equal volumes of the diluted sample and a 2% ammonium molybdate solution were combined and left for 3 min. A drop of this solution was placed on a copper mesh for 5 min before the excess liquid was drawn off using filter paper. The mesh was examined using a Philips 201C transmission electron microscope (Eindhoven, Netherlands).

For the cryo-FESEM, samples were plunge-frozen in liquid propane and then frozen with slushy liquid nitrogen at −140 °C. The frozen samples were fractured with a knife on the Alto 2500 Cryo Stage (Gatan, Abingdon, U.K.) and freeze-etched by cycling the temperature from −140 to −90 °C and back to −140 °C. The exposed surface was coated with Au and Pd for 120 s and examined under the JSM-6700F field emission scanning EM (JEOL, Tokyo, Japan) using an acceleration voltage of 10 kV.

Determination of ζ Potential. To swamp the original differences in ionic strength and allow ζ potential to be measured under identical ionic conditions, liposome dispersions were prepared using 0.1 M NaCl and the pH was adjusted using 1 M HCl and 1 M NaOH. The samples were diluted as required using a 0.1 M NaCl solution that had also been adjusted to the specific pH. The ζ potential was measured using the Zetasizer 4 with an AZ104 cell. Five measurements of 25 s duration at 100 mV were used to measure the ζ potential at the stationary layer 14.63% of the capillary diameter in from the wall.

Phase Transition Temperature. The liposome dispersions were concentrated to ~20% phospholipid using Centrisart 1 19239E centrifugal filters (Sartorius, Goettingen, Germany) at 4000*g* for 4 h in a CentraMP4R centrifuge (International Equipment Co., Needham Heights, MA). The concentrated dispersions were filled into 1 cm³ ampules, and a CSC 4100 differential scanning calorimeter (Calorimetry Sciences Corporation, Spanish Fork, UT) used to scan from 0 to 60 °C at a rate of 1 °C/min.

3706 *J. Agric. Food Chem.,* Vol. 54, No. 10, 2006

Thompson et al.

Bilayer Thickness and Lamellarity. The liposome dispersions were concentrated to ~20% phospholipid as described above. The samples were transferred into glass capillary tubes (1.5 mm diameter, Charles Supper Co., Natick, MA), and the scattering pattern was measured during exposure to low-divergence Cu Kα radiation with a wavelength of 1.54 Å (Rigaku MicroMax007, microfocus rotating anode generator with Osmic multilayer confocal optics; Tokyo, Japan). The exposure time varied from 10 to 15 min, with separate samples of the liposome dispersions analyzed at 20 and 40 °C. The diffraction images were recorded on a RAxisIV++ image-plate detector (Rigaku, Fuji) placed 100−300 mm from the sample. Diffraction patterns were visualized and analyzed using CrystalClear software (version 1.3.6SP0, Rigaku-MSC).

The repeat distance between the lattice planes for each of the liposome dispersions was calculated within the CrystalClear software using eq 1

$$d = \frac{\lambda}{2 \sin\left(\frac{1}{2}\tan^{-1}\frac{x}{X}\right)} \quad (1)$$

where d is the repeat distance between the lattice planes, λ is the wavelength of the X-ray beam, x is the radius of the Debye ring, and X is the distance between the sample and the detector. The distance X is accurate to ±0.2 mm and was determined from diffraction patterns taken at different rotational settings of three-dimensional crystals.

Permeability. The membrane permeability of the various liposome dispersions will depend on the specific molecule diffusing through the bilayer. Pulsed-field-gradient NMR (PFG-NMR) can be used to observe the diffusion of molecules in solution. Waldeck et al. (*39*) were the first to use PFG-NMR to measure the permeability of liposome membranes. This method involves fitting the PFG-NMR experimental data to Karger's model of exchange between two compartments. It was recently found that this method could be expanded to incorporate a distribution of compartment sizes and allow the average liposome diameter to be estimated (*40*).

The PFG-NMR diffusion measurements were carried out between 20 and 40 °C using a Bruker Avance 500 MHz spectrometer with a 50 G cm^{-1} z-gradient. The gradient strength (g) ranged from 5 to 50 G cm^{-1} in 32 steps, with a gradient pulse width (δ) of 5 ms. Several measurements were taken for each sample, with Δ (equivalent to the diffusion time t_D, time interval between gradient pulses) values of 60, 80, 100, and 150 ms. The liposome dispersions used in this experiment had been prepared in distilled water to minimize signal interference from the buffer salts and sedimented at $100000g$ for 8 h. These samples were at pH 6.9, and PCS measurements indicated no significant difference in liposome size compared with dispersions prepared in imidiazole buffer. The pellet was resuspended in a small amount of distilled water and filled into NMR tubes. Initial results were compromised by the peak corresponding to the diffusion of the liposomes within the sample being significantly larger than the peak from the diffusion of the water molecules between the intra- and extraliposomal spaces. Small buds of cotton wool were placed in the bottom of the NMR tube and sufficient of the concentrated dispersions added to moisten the wool. This reduced the diffusion of the liposomes within the sample to close to zero and inhibited thermal convection.

Models were fitted to the PFG-NMR experimental data using the nonlinear least-squares regression analyses in Matlab (version 6.5, The Mathworks Inc.). For the two-compartment model with exchange, the fitted parameters were the intraliposomal fraction p_1, the extraliposomal space diffusivity D_2, intraliposomal exchange time τ_1, the volume-weighted mean liposome diameter R_0, and liposome size distribution deviation σ. The liposome size distribution was fitted to a volume-weighted log-normal distribution. The mean permeability was calculated with

$$P = R_0/3\tau_1$$

RESULTS

Characterization of Phospholipid Material. *Proximate Analysis.* The results of the proximate analysis of the phospho-

Table 1. Composition of Phospholipid Powders As Determined by Proximate Analysis

component	MFGM phospholipid fraction	soy phospholipid fraction
moisture (%)	5.6	3.8
ash (%)	14.8	5.7
calcium (mg/100 g)	5.8	3.6
magnesium (mg/100 g)	1.8	6.2
potassium (mg/100 g)	2060	415
sodium (mg/100 g)	810	<0.6
phosphorus (mg/100 g)	29.7	31.7
phospholipid (%)	74	79
triglycerides (%)	negligible	negligible
nitrogen (%)	2.4	1.1
nitrogen/phospholipid ratio	0.032	0.014
cholesterol (%)	0.032	not detected

Table 2. Phospholipid Classes Present in the MFGM and Soy Phospholipid Powders (Weight Percent)

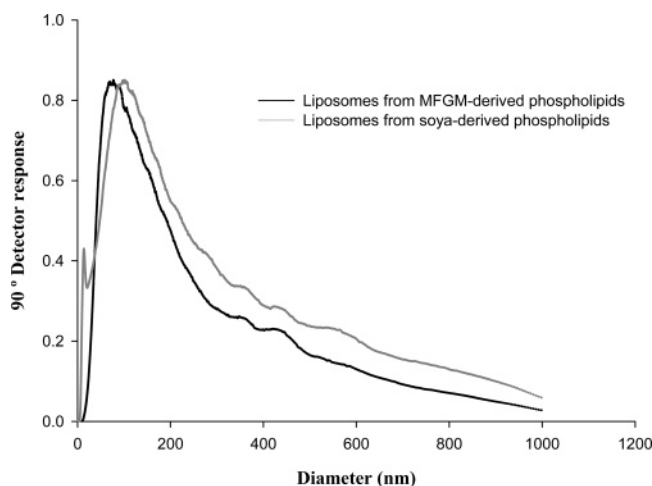| lipid	MFGM phospholipid fraction	soy phospholipid fraction
polar lipids	72.0	73.9
phosphatidyl choline	23.6	40.9
phosphatidyl ethanolamine	20.2	25.4
sphingomyelin	22.8	not detected
phosphatidyl serine	2.5	not detected
phosphatidyl inositol	2.6	3.6
other phospholipids	0.2	4.1

lipid fractions are shown in **Table 1**. The soy phospholipid material had less than half the ash content but a slightly higher phospholipid content than the MFGM phospholipid sample. The difference in the ash content was primarily due to the high levels of the monovalent cations (potassium and sodium) in the MFGM phospholipid fraction compared with the soy phospholipid fraction. The level of triglycerides present in either fraction was found to be negligible. The MFGM phospholipid fraction had over twice the nitrogen content of the soy phospholipid fraction, and the nitrogen/phospholipid ratio suggests a significantly higher protein level for the MFGM phospholipid sample. The cholesterol content of the MFGM phospholipid was negligible (0.032%), and no cholesterol was present in the soy fraction.

Phospholipid Headgroup. The phospholipid class composition of the phospholipid fractions is shown in **Table 2**. As expected on the basis of the phosphorus content, the two fractions had similar polar lipid contents, but the relative amounts of the specific phospholipid classes varied considerably. The MFGM material was primarily composed of approximately equal quantities of PC, PE, and SM, with small amounts of PI and PS. This is in agreement with the literature reports on the phospholipid composition of MFGM (*20, 27*). The soy phospholipid fraction had a significantly higher proportion of PC, with about one-third PE and a small amount of PI.

Fatty Acid Profile. There was a noticeable difference between the fatty acid profiles of the two fractions (**Table 3**). The animal origin of the MFGM phospholipid fraction was reflected in the higher percentage of saturated and mono-unsaturated fatty acids, whereas the soy-derived fraction contained more poly-unsaturated fatty acids. The differences between the measured and the literature values for the soy material is likely to be due to the literature referring to soy oil, rather than a soy phospholipid extract. As discussed in our earlier paper (*26*), the MFGM values are similar to those reported by Fauquant et al. (*41*), with the

Structure and Properties of Liposomes

J. Agric. Food Chem., Vol. 54, No. 10, 2006   **3707**

Table 3. Comparison between the Fatty Acid Content of the Phospholipid Powders and the Literature Values for the Source of Each Fraction

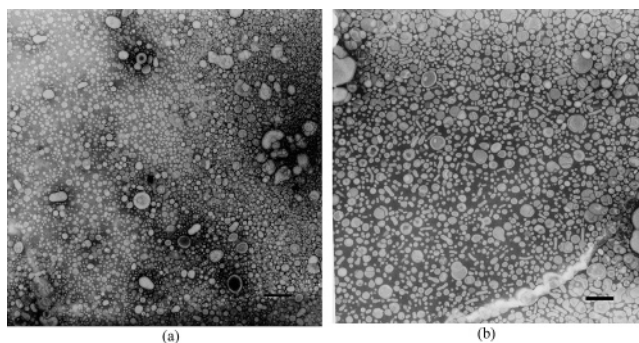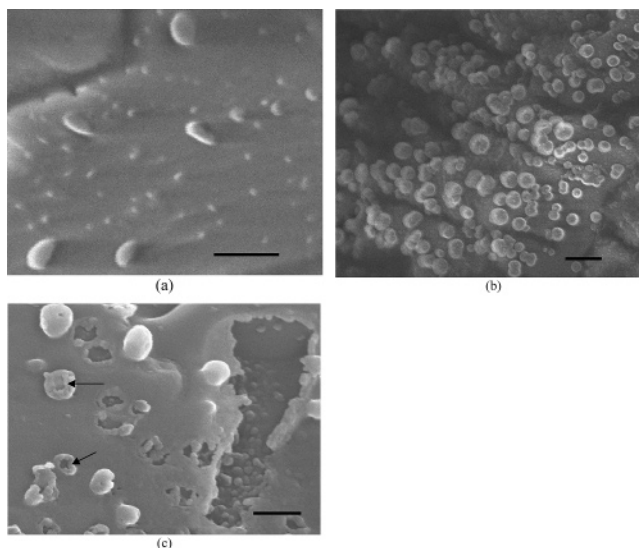| fatty acid	phospholipid fraction (wt %)		literature values (wt %)	
	MFGM	soy	MFGM (*41*)	soybean oil (*64*)
C14:0	3.1	0.1	1.9–2.2	trace
C16:0	16.2	15.6	16.5–19.4	11
C16:1	1.4	0.2	1.2–1.6	trace
C18:0	10.0	3.7	16.3–17.9	4
C18:1	30.3	8.6	27.7–30.7	22
C18:2n–6	4.8	57.5	6.1–6.9	53
C18:3n–3	1.8	7.5	0.4–0.6	8
C20:2n–6	0.5	0.3	0.5–1.5	trace
C20:3n–6	0.7	0.0	1.0–1.3	trace
C20:4n–6	0.7	0.1	0.9–2.2	trace
C20:5n–3	0.6	0.0	0.2–0.6	trace
C22:0	4.2	0.2	3.5–4.8	trace
C22:5n–3	1.0	0.0	0.5–0.6	trace
C22:5n–6	6.5	0.2	0.3–0.5	trace
C24:0	4.0	0.2	3.1–3.9	trace

Figure 2. Negative staining TEM micrographs of liposomes produced via microfluidization from the (**a**) MFGM and (**b**) soy phospholipid fractions. Bar = 0.5 μm.

Figure 3. Cryo-FESEM micrographs of liposomes produced via microfluidization from the (**a**) MFGM and (**b**, **c**) soy phospholipid fractions: (**c**) structures consistent with liposomes—an internal cavity surrounded by an outer shell. Bar = 0.2 μm in (**a**) and (**b**) and 0.1 μm in (**c**).

Figure 1. Normalized 90° detector response for specified liposome diameters on a linear scale as determined by asymmetric field flow fractionation.

higher proportion of C22:5 fatty acid chains possibly a consequence of the selective removal of buttermilk components during fractionation.

Characterization of Liposomes Produced from Phospholipid Material. *Average Size and Distribution of Liposomes within the Dispersions.* The average hydrodynamic diameters of liposome dispersions produced by five passes through the Microfluidizer at 1100 bar were 95 ± 5 and 81 ± 5 nm for the MFGM phospholipid and soy phospholipid dispersions, respectively. All samples had high polydispersity values (~0.5), indicating a very wide particle size distribution. These results are similar to previous reports of liposomes produced by microfluidization, with an average diameter of 100−200 nm and a polydispersity of between 0.2 and 0.6 (*1*).

Possible size distributions as determined by asymmetric field flow fractionation (AFFF) showed that liposomes made from both of the phospholipid fractions had a primary peak at ~100 nm, with a long tail stretching past 1000 nm (**Figure 1**). The length of this tail is in agreement with polydispersity values obtained by the Zetasizer. The soy phospholipid dispersion also appeared to have a small peak at ~15 nm. This is smaller than the 20−25 nm theoretical minimum liposome diameter (*12*). This minimum is based on assumptions regarding thickness of

the bilayer (*42*) and overcrowding of phospholipid headgroups caused by surface curvature (*32*). It has been suggested that microfluidization may produce micelle-like structures (*43*), but other workers have refuted this (*44*). Assuming that the micelle is composed of a monolayer of phospholipid molecules with the hydrophobic fatty acid chains touching in the middle, its diameter would be approximately the same as the thickness of the bilayer. An average membrane thickness for liposomes of ~4 nm has been reported (*42*), which is too small for micelles to be responsible for the peak at 15 nm. A glycerol density gradient used to separate bands of liposomes from a number of dispersions revealed that 76% of the liposomes present in one dispersion were smaller than 22 nm in diameter and that 63% had diameters of between 11 and 19 nm (*45*). Therefore, it seems probable that the small particles observed using AFFF were indeed very small liposomes.

Electron Microscopy. Negative staining TEM micrographs of the two liposome dispersions are shown in **Figure 2**, with micrographs produced by cryo-FESEM shown in **Figure 3**. The liposomes could easily be identified as discrete particles that were predominantly spherical or rodlike in shape. The particles ranged in size from ≤40 nm to between 100 and 200 nm in diameter. This is in line with the size distribution suggested by the PCS and AFFF results.

The negative staining TEM allowed the outer membrane surrounding the internal aqueous space to be clearly seen in many of the liposomes, and internal membranous structures could also be identified. Most large heterogeneous liposome systems typically contain liposomes with irregularly spaced bilayers or "liposome within liposome" structures (*46*), often referred to as multivesicular liposomes (*47*, *48*). This is in contrast with the common assumption that multilamellar liposomes are composed of neatly stacked lamellae at regular spacing. Freeze−fracture TEM micrographs of liposomes produced via microfluidization have shown irregularly shaped vesicles trapped inside other vesicles (*44*), as do those formed from phospholipid pastes produced by high-pressure homogenization (*48*).

The cryo-field emission SEM provided three-dimensional confirmation of the liposome structure, showing smooth spherical structures, some of which were broken during the preparation process to reveal an internal space that had been fully enclosed by an outer shell (**Figure 3c**).

ζ Potential. The ζ potentials of the MFGM phospholipid liposome dispersions at pH 6.0 and 7.0 were −64 ± 2.0 and −67 ± 2.5 mV, respectively. The soy phospholipid liposome dispersion had higher ζ potentials, −77 mV ± 1.5 at pH 6.0 and −79 ± 1.3 mV at pH 7.0. The negative ζ potential presumably reflects the presence of negatively charged phospholipids, particularly PI. Charge neutralization and the presence of proteins will also influence the ζ potential, and the slightly higher proportion of PI and lower concentration of cations in the soy material may help explain its larger negative charge.

Phase Transition Temperature. The differential scanning calorimeter thermogram showed a broad endothermic peak between 20 and 35 °C for the MFGM phospholipid liposome dispersion, with the peak at ∼28 °C. This is likely to correspond to the bilayer membranes transforming from gel to liquid-crystal state. There were no significant features present between 0 and 60 °C in the liposome dispersions made from the soy phospholipid, indicating that the phase transition temperature was below 0 °C. These results were as expected on the basis of the origin of the phospholipid fractions. Nonhydrogenated soy phospholipids usually undergo phase transition between −15 and −5 °C, whereas phospholipids from animal sources have phase transition temperatures above 0 °C (*12*). Milk sphingomeylin has been reported as having a T_c of 35 °C at concentrations of <70 wt % (*49*).

The width of the observed endothermic peak reflects the complicated mixture of phospholipid classes and types of fatty acids present in the fraction (*50*, *51*) and is similar to endotherms obtained for biological membranes (*52*). Each different combination of headgroup and fatty acid will have a slightly different phase transition temperature, resulting in the coexistence of gel and fluid phases and a total phase transition over a wide range of temperatures (*53*).

Bilayer Thickness. The small-angle X-ray diffraction of the samples at 20 °C showed broad single peaks with diffraction maxima (indicative of membrane thickness) of 68 and 52 Å for the MFGM phospholipid and soy phospholipid dispersions, respectively. The MFGM liposomes had a membrane thickness of ∼15 Å larger than that of the soy phospholipid liposomes. These measurements were made at 20 °C, which was above the phase transition temperature for the soy fraction but below the transition temperature for the MFGM bilayer. Examination of samples at 40 °C (above the phase transition temperature for both samples) showed no significant change in bilayer thickness for the soy phospholipid fraction, but the MFGM

bilayer thickness reduced by 3 Å to 65 Å, possibly due to the change in membrane state.

Marsh (*53*) stated that the lipid bilayer is "considerably" thinner in the fluid state than in the gel state but did not give an indication of the actual numerical size of this change, whereas Malmsten et al. (*49*) commented that the repeat distance of the lamellar phase for milk sphingomyelin changed by <5 Å between the gel and fluid phases.

Lamellarity. Small-angle X-ray diffraction may also be used to provide an indication of the lamellarity of a liposome population (*54*). X-ray scattering curves from dispersions containing only unilamellar liposomes are typically very broad and flat, and usually have only a single symmetric peak. Those from multilamellar liposomes exhibit first- and second-order diffraction peaks at regular intervals, that is, 1/d, 2/d, etc. (*55*−*57*).

A primarily unilamellar population with a small number of bi- or trilamellar vesicles is likely to result in a broad, asymmetric peak (*54*), similar to that obtained from these samples (data not shown). This observation is also in agreement with the negative staining TEM micrographs shown in **Figure 3**, which appear to indicate a primarily unilamellar population with a small number of multilamellar and multivesicular liposomes. Bouwstra et al. (*54*) stated that if the majority of the multilamellar liposomes present in a system are only bi- or trilamellar, they will need to constitute a significant proportion (>20%) of the total liposome population before they will have a clear effect on the X-ray scattering curve. Multilamellar liposomes that have different lamellar spacings either within the same vesicle or between different vesicles will have different diffraction patterns, which may average out to a broad smooth peak (*57*), and any multivesicular liposomes will respond as unilamellar structures (*47*). Therefore, it is not possible to determine whether the broad single peak observed corresponds to unilamellar or multivesicular liposomes or to quantify the specific quanity of multilamellar liposomes present in the dispersions.

Permeability. The first step in determining the permeability of water through the bilayer was to confirm that there was indeed exchange between the water trapped inside the liposome and the bulk aqueous phase. This can be done by comparing the experimental diffusion pattern with model predictions with and without exchange between two compartments. **Figure 4** shows plots of the relative signal attenuation for the water peak for values of Δ between 60 and 150 using both the model that is based on no exchange between compartments and the model that assumes some exchange will be taking place. When these plots are compared with the experimental data obtained from the liposome dispersions, it is obvious that the model that includes exchange provides a much closer fit to the actual results. Similar plots were observed for sucrose.

The PFG-NMR results showed that water diffused through a liposome membrane made from the soy phospholipid material at ∼$4.7E^{-06}$ m/s, 3 times faster than it was able to permeate membranes composed of the MFGM phospholipid fraction (**Table 4**). These values compared well with previously reported values of $3-6E^{-6}$ m/s (*46*) and E^{-5} m/s (*58*). Increasing the temperature from 20 to 40 °C had no effect on the permeability of the liposome membranes made from the soy phospholipid. There was no noticeable change in permeability across this temperature range for the MFGM phospholipid dispersion, and there was no increase at the phase transition temperature (28−30 °C).

The results suggest that there is only a minimal effect of membrane phase or phase transition on the permeability of the
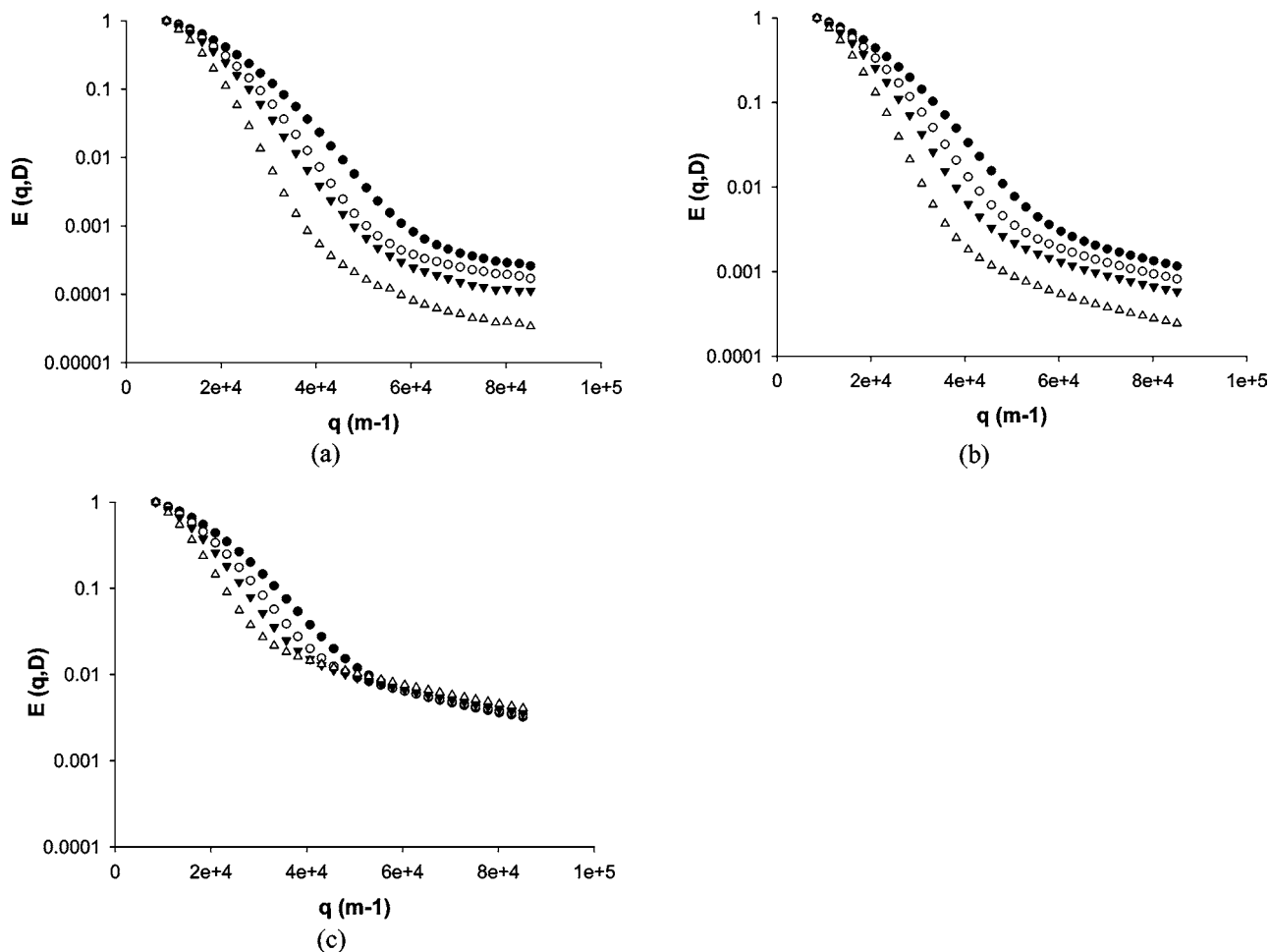
Structure and Properties of Liposomes

J. Agric. Food Chem., Vol. 54, No. 10, 2006 **3709**

(a)

(b)

(c)

Figure 4. Plots of the relative signal attenuation for the water peak measured using PFG-NMR: (**a**) model with no exchange, $a = 5E^{-7}$, sigma = 0.8, p1 = 0.05, Diff = 1e^{-9} m/s; (**b**) model with exchange, $a = 5E^{-7}$, sigma = 0.8, p1 = 0.05, t1 = 0.05 s, Diff = 1e^{-9} m/s; (**c**) typical response for liposome dispersions (actual data from a MFGM phospholipid dispersion). Δ (equivalent to the diffusion time t_D, time interval between gradient pulses) values of 60 (●), 80 (○), 100 (▼), and 150 (▽) were used.

Table 4. Effect of Temperature on the Membrane Permeability of Water through Liposomes Produced from Each of the Phospholipid Fraction

	mean permeability of water through the liposome membrane (m/s)			
phospholipid fraction	20 °C	28 °C	30 °C	40 °C
MFGM	$1.6E^{-06} \pm 3.0E^{-07}$	$1.5E^{-06} \pm 3.0E^{-07}$	$1.4E^{-06} \pm 2.8E^{-07}$	$1.2E^{-06} \pm 2.4E^{-07}$
soy	$4.7E^{-06} \pm 9.4E^{-07}$			$4.8E^{-06} \pm 9.6E^{-07}$

MFGM liposome membranes to small molecules such as water. Previous studies indicate that the permeability of the membrane should be highest at the phase transition temperature (*32*), but there was no indication of such increase at 28 or 30 °C for the MFGM fraction. The presence of high concentrations of cholesterol can reduce or remove evidence of this transition (*12, 32, 59*). The MFGM material contained <0.05% cholesterol (**Table 1**), which was probably too low to have any significant effect. Reineccius (*12*) and Frezard (*60*) stated that the transformation of the MFGM-derived phospholipid membrane from the gel to the liquid-crystal phase would result in an increase in membrane permeability as the packing density of the membrane decreases, but the experimental data showed a small decrease in measured permeability. However, this observation corresponds with the slight reduction in bilayer thickness determined using small-angle X-ray diffraction. The increase in temperature did not change the phase of the soy phospholipid membranes, and so the lack of a significant effect of the temperature on permeability was as expected.

DISCUSSION

The most significant differences between the phospholipid compositions were the high level of sphingomyelin in the MFGM phospholipid fraction (approximately one-third of the polar lipid present) and the higher degree of saturation of the fatty acid chains. Sphingomyelin has a more structured gel phase than PC, and sphingomyelin membranes seem to be more stable and have a lower permeability to hydrophilic molecules than PC bilayers (*61*). Phospholipids composed of saturated fatty acids tend to be less susceptible to oxidation than their unsaturated counterparts and may reduce the membrane permeability due to their ability to pack more tightly within the membrane (*62*).

MFGM material appeared to contain a slightly higher level of protein than the soy fraction. The amphipathic nature of protein means the protein molecules are likely to become incorporated in the phospholipid membrane, with hydrophobic portions located in the interior of the bilayer and the hydrophilic

portions in the aqueous phase either inside or outside the liposome. Therefore, the protein present in the dispersion has either been incorporated into the membrane during liposome formation or become adsorbed to the surface of the membrane postformation. In biological systems, proteins rapidly adsorb to the liposome membrane (*7, 63*). Steric and charge repulsion forces are likely to cause at least some part of the hydrophilic portion of the proteins to extend from the membrane surface. Shi et al. (*65*) found that coating liposomes with collagen or polysaccharide material such as chitosan significantly decreased membrane permeability. Although there is no previous information regarding the use of dairy or soy proteins in this situation, it is probable that proteins from other sources would have similar effects. Thus, the presence of proteins within the hydrophobic interior of the membrane and/or as an additional barrier on the liposome surface may be responsible for the increased membrane thickness for the MFGM phospholipid liposomes, as well as their reduced membrane permeability for water. It is well-known that the presence of sterols within the liposome membrane can prevent the increase in permeability observed during phase transition (*32*), and it is possible that protein material within the membrane structure may also affect the behavior of the membrane during phase transition.

On the basis of the measured ζ potentials, it would be expected that liposomes produced from the soy phospholipid fraction would have a higher level of charge repulsion compared with liposomes produced from the MFGM phospholipid fraction. These repulsions may increase the resistance of soy phospholipid liposome dispersions to aggregation or coalescence between pH 6 and 7. However, despite the MFGM membranes' being less strongly charged, the presence of sphingomyelin may provide a different mechanism for enhancing the stability of these liposome dispersions. Further studies will be undertaken to compare the stability of liposomes produced from the soya and MFGM fractions in a range of conditions. If the MFGM phospholipid liposomes demonstrate good stability characteristics in addition to their lower membrane permeability, they would provide a number of potential advantages over the traditional soy phospholipids in the delivery of bioactives in food systems.

LITERATURE CITED

(1) Zeisig, R.; Cämmerer, B. Liposomes in the food industry. In *Microencapsulation of Food Ingredients*; Vilstrup, P., Ed.; Leatherhead Publishing: Surrey, U.K., 2001; pp 101−119.

(2) Lasic, D. D. Novel applications of liposomes. *Trends Biotechnol.* **1998**, *16*, 307−321.

(3) Arnaud, J.-P. Liposomes in the agro/food industry. *Agro-Food Ind. Hi-Tech* **1995**, Sept/Oct, 30−36.

(4) Augustin, M.; Sanguansri, L.; Margetts, C.; Young, B. Microencapsulation of food ingredients. *Food Aust.* **2001**, *53*, 220−223.

(5) Hawker, N.; Ghyczy, M. Liposomes for the food industry (ingredients interview). *Food Technol. Eur.* **1994**, 44−46.

(6) Jackson, L. S.; Lee, K. Microencapsulation and the food industry. *Lebensm. Wiss. Technol.* **1991**, *24*, 289−297.

(7) Keller, B. Liposomes in nutrition. *Trends Food Sci. Technol.* **2001**, *12*, 25−31.

(8) Kirby, C. Microencapsulation and controlled delivery of food ingredients. *Food Sci. Technol. Today* **1991**, *5*, 74−78.

(9) Kirby, C. J.; Whittle, C. J.; Rigby, N.; Coxon, D. T.; Law, B. A. Stabilization of ascorbic acid by microencapsulation in liposomes. *Int. J. Food Sci. Technol.* **1991**, *26*, 437−449.

(10) Laridi, R.; Kheadr, E.; Benech, R.; Vuillemard, J.; Lacroix, C.; Fliss, I. Liposome encapsulated nisin Z: optimization, stability and release during milk fermentation. *Int. Dairy J.* **2003**, *13*, 325−336.

(11) Puisieux, F.; Couvreur, P.; Delattre, J.; Devissaquet, J.-P. In *Liposomes, New Systems and New Trends in Their Application*; Editions de Sante: Paris, France, 1995.

(12) Reineccius, G. Liposomes for controlled release in the food industry. In *Encapsulation and Controlled Release of Food Ingredients*; Risch, S., Reineccius, G., Eds.; American Chemical Society: Washington, DC, 1995; pp 113−131.

(13) Thompson, A. Liposomes: from concept to application. *Food New Zealand* **2003**, *Feb/March*, S23−S32.

(14) Weiner, N. Phospholipid liposomes: properties and potential use in flavor encapsulation. In *Flavor Technology*; ACS Symposium Series; American Chemical Society: Washington, DC, 1995; pp 210−218.

(15) Best, D. Ingredient trends alert. *Food Process.* **2000**, 57−62.

(16) Koopman, J.; Turkish, V.; Monto, A. Infant formula and gastrointestinal illness. *Am. J. Public Health* **1985**, *75*, 477−480.

(17) Crook, T.; Tinklenberg, J.; Yesavage, J.; Petrie, W.; Nunzi, M.; Massari, D. Effects of phosphatidylserine in age-associated memory impairment. *Neurology* **1991**, *41*, 644−649.

(18) Crook, T.; Petrie, W.; Wells, C.; Massari, D. Effects of phosphatidylserine in Alzheimer's disease. *Psychopharmacol. Bull.* **1992**, *28*, 61−66.

(19) Peel, M. Liposomes produced by combined homogenization/extrusion. *GIT Lab. J.* **1999**, *3*, 37−38.

(20) Astaire, J. C.; Ward, R.; German, J. B.; Jimenez-Flores, R. Concentration of polar MFGM lipids from buttermilk by microfiltration and supercritical fluid extraction. *J. Dairy Sci.* **2003**, *86*, 2297−2307.

(21) Corredig, M.; Roesch, R. R.; Dalgleish, D. G. Production of a novel ingredient from buttermilk. *J. Dairy Sci.* **2003**, *86*, 2744−2750.

(22) Corredig, M.; Dalgleish, D. G. Characterization of the interface of an oil-in-water emulsion stabilized by milk fat globule membrane material. *J. Dairy Res.* **1998**, *65*, 465−477.

(23) Roesch, R. R.; Rincon, A.; Corredig, M. Emulsifying properties of fractions prepared from commercial buttermilk by microfiltration. *J. Dairy Sci.* **2004**, *87*, 4080−4087.

(24) Yuasa, H.; Sekiya, M.; Ozeki, S.; Watanabe, J. Evaluation of milk fat-globule membrane (MFGM) emulsion for oral administration: absorption of alpha-linolenic acid in rats and the effect of emulsion droplet size. *Biol. Pharm. Bull.* **1994**, *17*, 756−758.

(25) Sato, H.; Liu, H.; Adachi, I.; Ueno, M.; Lemaire, M.; Horikoshi, I. Enhancement of the intestinal absorption of a cyclosporine derivative by milk fat globule membrane. *Biol. Pharm. Bull.* **1994**, *17*, 1526−1528.

(26) Thompson, A.; Singh, H. Preparation of liposomes from milk fat globule membrane phospholipids using a microfluidiser. *J. Dairy Sci.* **2006**, *89*, 410−419.

(27) Boyd, L. C.; Drye, N. C.; Hansen, A. P. Isolation and characterization of whey phospholipids. *J. Dairy Sci.* **1999**, *82*, 2550−2557.

(28) Schneider, M. Phospholipids. In *Lipid Synthesis and Manufacture*; Gunstone, F. D., Ed.; Sheffield Academic Press: Sheffield, U.K., 1999; pp 51−78.

(29) Cerbulis, J.; Parks, O.; Farrell, J. Fatty acid composition of polar lipids in goats' milk. *Lipids* **1983**, *18*, 55−58.

(30) Waninge, R.; Nylander, T.; Paulsson, M.; Bergenstahl, B. Milk membrane lipid vesicle structures studied with Cryo-TEM. *Colloids Surf. B* **2003**, *31*, 257−264.

(31) Jousma, H.; Talsma, H.; Spies, F.; Joosten, J.; Junginger, H.; Crommelin, D. Characterization of liposomes. The influence of extrusion of multilamellar vesicles through polycarbonate membranes an particle size, particle size distribution and number of bilayers. *Int. J. Pharm.* **1987**, *35*, 263−274.

(32) New, R. Introduction. In *Liposomes—a Practical Approach*; New, R., Ed.; IRL Press: Oxford, U.K., 1990; pp 1−32.

(33) Asther, M.; Record, E.; Antona, C.; Asther, M. Increased phospholipid transfer protein activity in *Aspergillus oryzae* grown on various industrial phospholipid sources. *Can. J. Microbiol.* **2001**, *47*, 685−689.

Structure and Properties of Liposomes

J. Agric. Food Chem., Vol. 54, No. 10, 2006 **3711**

(34) Alvarado, I.; Navarro, D.; Record, E.; Asther, M.; Lesage-Meessen, L. Fungal biotransformation of *p*-coumaric acid into caffeic acid by *Pycnoporus cinnabarinus*: an alternative for producing a strong natural antioxidant. *World J. Microbiol. Biotechnol.* **2003**, *19*, 157−160.

(35) Diehl, B. ^{31}P NMR in study of phosphorous containing lipids. *Lipid Technol.* **2002**, *14*, 62−65.

(36) Diehl, B. High-resolution NMR spectroscopy. *Eur. J. Lipid Sci. Technol.* **2001**, *103*, 16−20.

(37) Ardhammer, M.; Lincoln, P.; Norden, B. Invisible liposomes: refractive index matching with sucrose enables flow dichroism assessment of peptide orientation in lipid vesicle membrane. *Proc. Natl. Acad. Sci. U.S.A.* **2002**, *99*, 15313−15317.

(38) Blessing, T.; Remy, J.-S.; Behr, J.-P. Monomolecular collapse of plamid DNA into stable virus-like particles. *Proc. Natl. Acad. Sci. U.S.A.* **1998**, *95*, 1427−1431.

(39) Waldeck, A. R.; Kuchel, P. W.; Lennon, A. J.; Chapman, B. E. NMR diffusion measurements to characterise membrane transport and solute binding. *Prog. Nucl. Magn. Reson. Spectrosc.* **1997**, *30*, 39−68.

(40) Hindmarsh, J. P.; Su, J.; Flanagan, J.; Singh, H. PFG-NMR Analysis of intercompartment exchange and inner droplet size distribution of W/O/W emulsions. *Langmuir* **2005**, *21*, 9076−9084.

(41) Fauquant, C.; Briard, V.; Leconte, N.; Michalski, M. Differently sized native milk fat globules separated by microfiltration: fatty acid composition of the milk fat globule membrane and triglyceride core. *Eur. J. Lipid Sci. Technol.* **2005**, *107*, 80−86.

(42) Watwe, R.; Bellare, J. Manufacture of liposomes: a review. *Curr. Sci. India* **1995**, *68*, 715−724.

(43) Lasic, D. D. *Liposomes: From Physics to Applications*; Elsevier: New York, 1993.

(44) Škalko, N.; Bouwstra, J.; Spies, F.; Stuart, M.; Frederik, P.; Gregoriadis, G. Morphological observations on liposomes bearing covalently bound protein: studies with freeze-fracture and cryo electron microscopy and small-angle X-ray scattering techniques. *Biochim. Biophys. Acta* **1998**, *1370*, 151−160.

(45) Goormaghtigh, E.; Scarborough, G. Density-based liposome sizing by glycerol gradient centrifugation. In *Liposome Technology*; Gregoriadis, G., Ed.; CRC Press: Boca Raton, FL, 1993; pp 315−330.

(46) Perkins, W. M., S.; Ahl, P.; Janoff, A. The determination of liposome captured volume. *Chem. Phys. Lipids* **1993**, *64*, 197−217.

(47) Talsma, H.; Jousma, H.; Nicolay, K.; Lasic, D. Multilamellar or multivesicular vesicles? *Int. J. Pharm.* **1987**, *37*, 171−173.

(48) Brandl, M.; Drechsler, M.; Bachmann, D.; Tardi, C.; Schmidtgen, M.; Bauer, K.-H. Preparation and characterization of semi-solid phospholipid dispersions and dilutions thereof. *Int. J. Pharm.* **1998**, *170*, 187−199.

(49) Malmsten, M.; Bergenstahl, B.; Nyberg, L.; Odham, G. Sphingomyelin from milk−characterisation of liquid crystalline, liposome and emulsion properties. *J. Am. Oil Chem. Soc.* **1994**, *17*, 1021−1026.

(50) Lee, A. Lipid phase transitions and phase diagrams: I. Lipid phase transitions. *Biochim. Biophys. Acta* **1977**, *472*, 237−281.

(51) Lee, A. Lipid phase transitions and phase diagrams: II. Mixtures involving lipids. *Biochim. Biophys. Acta* **1977**, *472*, 285−344.

(52) McElhaney, R. The suitability of liposomes as models for studying lipid phase transitions and lipid organization and dynamics in biological membranes. In *The Handbook of Nonmedical Applications of Liposomes*; Barenholz, Y., Lasic, D., Eds.; CRC Press: Boca Raton, FL, 1996; pp 21−49.

(53) Marsh, D. Physical characterization of liposomes for understanding structure−function relationships in biological membranes. In *Handbook of Nonmedical Applications of Liposomes*; Barenholz, Y., Lasic, D., Eds.; CRC Press: Boca Raton, FL, 1996; pp 1−19.

(54) Bouwstra, J.; Gooris, G.; Bras, W.; Talsma, H. Small-angle X-ray scattering: possibilities and limitations in characterisation of vesicles. *Chem. Phys. Lipids* **1993**, *64*, 83−98.

(55) Hauser, H. Phospholipid vesicles. In *Phospholipids Handbook*; Cevc, G., Ed.; Dekker: New York, 1993; pp 603−637.

(56) Kinnunen, P.; Alakoskela, J.-M.; Laggner, P. Phase behaviour of liposomes. *Methods Enzymol.* **2003**, *367*, 129−147.

(57) Moody, M. Studying liposomes by X-ray scattering. In *Liposome Technology*; Gregoriadis, G., Ed.; CRC Press: Boca Raton, FL, 1993; pp 385−397.

(58) Epand, R.; Polozov, I. Liposomes and membrane stability. In *Handbook of Nonmedical Applications of Liposomes*; Barenholz, Y., Lasic, D., Eds.; CRC Press: Boca Raton, FL, 1996; pp 105−111.

(59) Lian, T.; Ho, R. J. Trends and developments in liposome drug delivery systems. *J. Pharm. Sci.* **2001**, *90*, 667−680.

(60) Frezard, F. Liposomes: from biophysics to the design of peptide vaccines. *Braz. J. Med. Biol. Res.* **1999**, *32*, 181−189.

(61) New, R. Preparation of liposomes. In *Liposomes−a Practical Approach*; New, R., Ed.; IRL Press: Oxford, U.K., 1990; pp 33−104.

(62) Monroig, O. N. J.; Amat, I.; Gonzalez, P.; Amat, F.; Hontoria, F. Enrichment of *Artemia nauplii* in PUFA, phospholipids, and water-soluble nutrients using liposomes. *Aquacult. Int.* **2003**, *11*, 151−161.

(63) Juliano, R.; Meyer, M. Interactions of lipid membranes with blood cells and proteins: implications for drug delivery and for biocompatibility. In *Liposome Technology*; Gregoriadis, G., Ed.; CRC Press: Boca Raton, FL, 1993; pp 15−25.

(64) Gurr, M.; Harwood: J.; Frayn, K. *Lipid Biochemistry*, 5th ed.; Blackwell: London, U.K., 2002.

(65) Shi, X.-Y.; Sun, C.-M.; Wu, S.-K. Evaluation of in vitro stability of small unilamellar vesicles coated with collagen and chitosan. *Polym. Int.* **1999**, *48*, 212−216.